Gamma-ray spectroscopy IV

Andreas Görgen
DAPNIA/SPhN, CEA Saclay
F-91191 Gif-sur-Yvette
France
agoergen@cea.fr

Lectures presented at the
IoP Nuclear Physics Summer School
September 4 – 17, 2005
Chester, UK

dapnia SPhN
cea
saclay

Outline

First lecture
- Properties of γ-ray transitions
- Fusion-evaporation reactions
- Germanium detector arrays
- Coincidence technique
- Nuclear deformations
- Rotation of deformed nuclei
- Pair alignment
- Superdeformed nuclei
- Hyperdeformed nuclei
- Triaxiality and wobbling

Second lecture
- Angular distribution
- Linear polarization
- Jacobi shape transition
- Charged-particle detectors
- Neutron detectors
- Prompt proton decay
- Recoil-decay tagging
- Rotation and deformation alignment

Third lecture
- Spectroscopy of transfermium nuclei
- Conversion-electron spectroscopy
- Quadrupole moments and transition rates
- Recoil-distance method
- Doppler shift attenuation method
- Fractional Doppler shift method
- Magnetic moments
- Perturbed angular distribution
- Magnetic Rotation
- Shears Effect

Fourth lecture
- Fast fragmentation beams
- Isomer spectroscopy after fragmentation
- E0 transitions
- Shape coexistence
- Two-level mixing
- Coulomb excitation
- Reorientation effect
- ISOL technique
- Low-energy Coulomb excitation of ^{74}Kr
- Relativistic Coulomb excitation of ^{58}Cr
- Gamma-ray tracking
- AGATA

Summary (III)

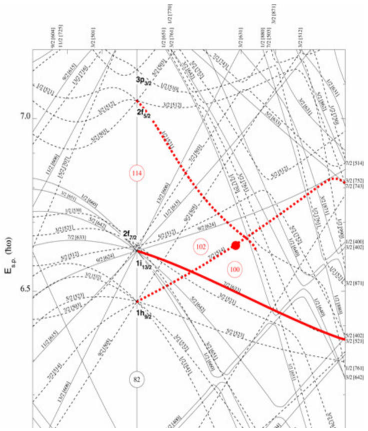

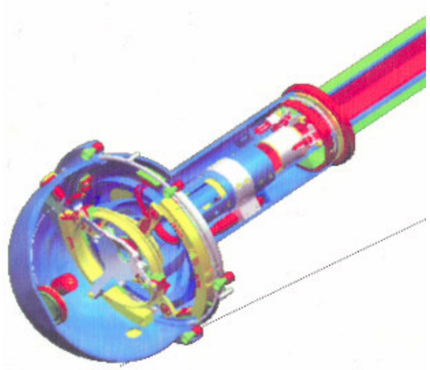

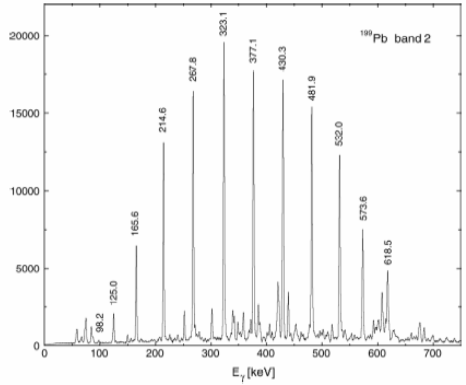
^{199}Pb band 2
98.2
125.0
165.6
214.6
267.8
323.1
377.1
430.3
481.9
532.0
573.6
618.5
E_γ [keV]

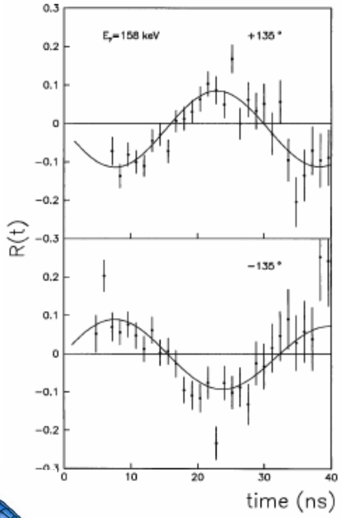
E_γ=158 keV
+135°
−135°
R(t)
time (ns)

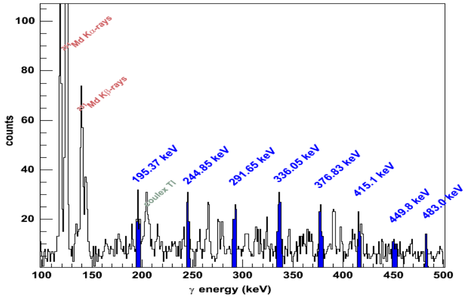
counts
195.37 keV
244.85 keV
291.65 keV
336.05 keV
376.83 keV
415.1 keV
449.8 keV
483.0 keV
γ energy (keV)

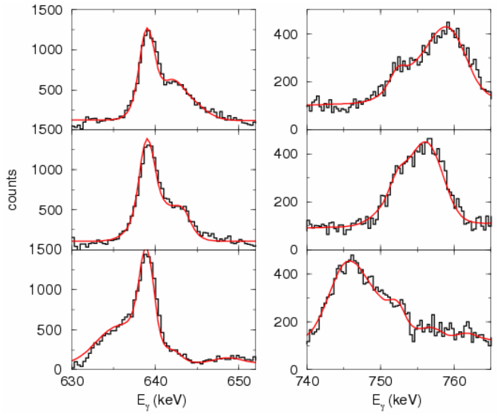
counts
E_γ (keV)
E_γ (keV)

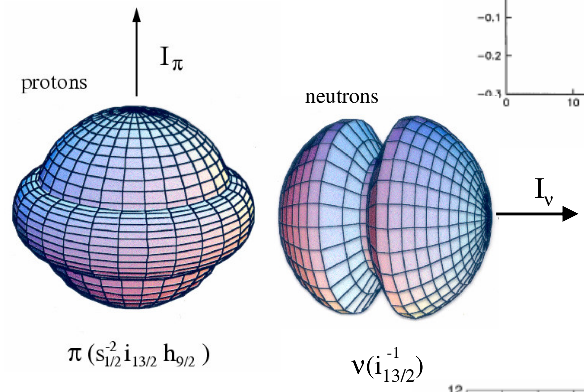
protons
I_π
neutrons
I_ν
$\pi (s_{1/2}^{-2}\, i_{13/2}\, h_{9/2})$
$\nu(i_{13/2}^{-1})$

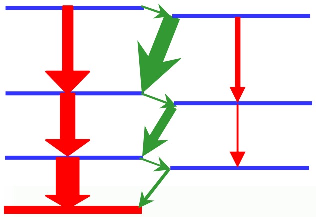

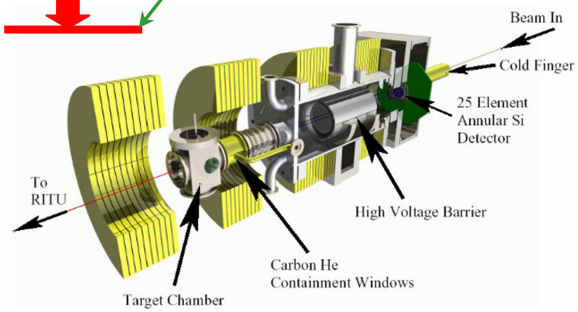
Beam In
Cold Finger
25 Element
Annular Si
Detector
To
RITU
High Voltage Barrier
Carbon He
Containment Windows
Target Chamber

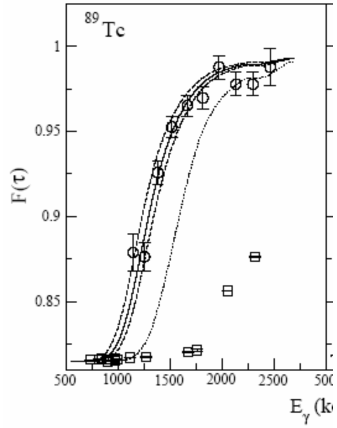
^{89}Tc
F(τ)
E_γ

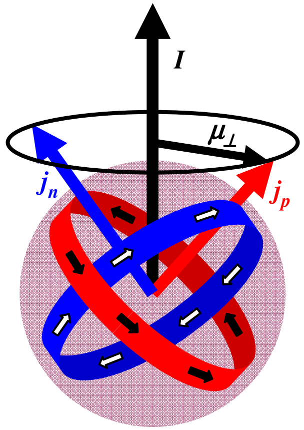
I
$\mu_\perp$
j_n
j_p

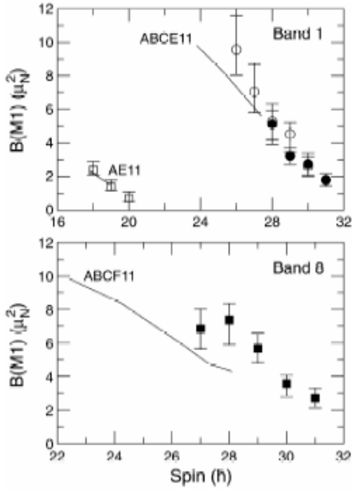
Band 1
ABCE11
AE11
B(M1) (μ_N^2)
Band 8
ABCF11
Spin (ħ)

Fast fragmentation beams: production

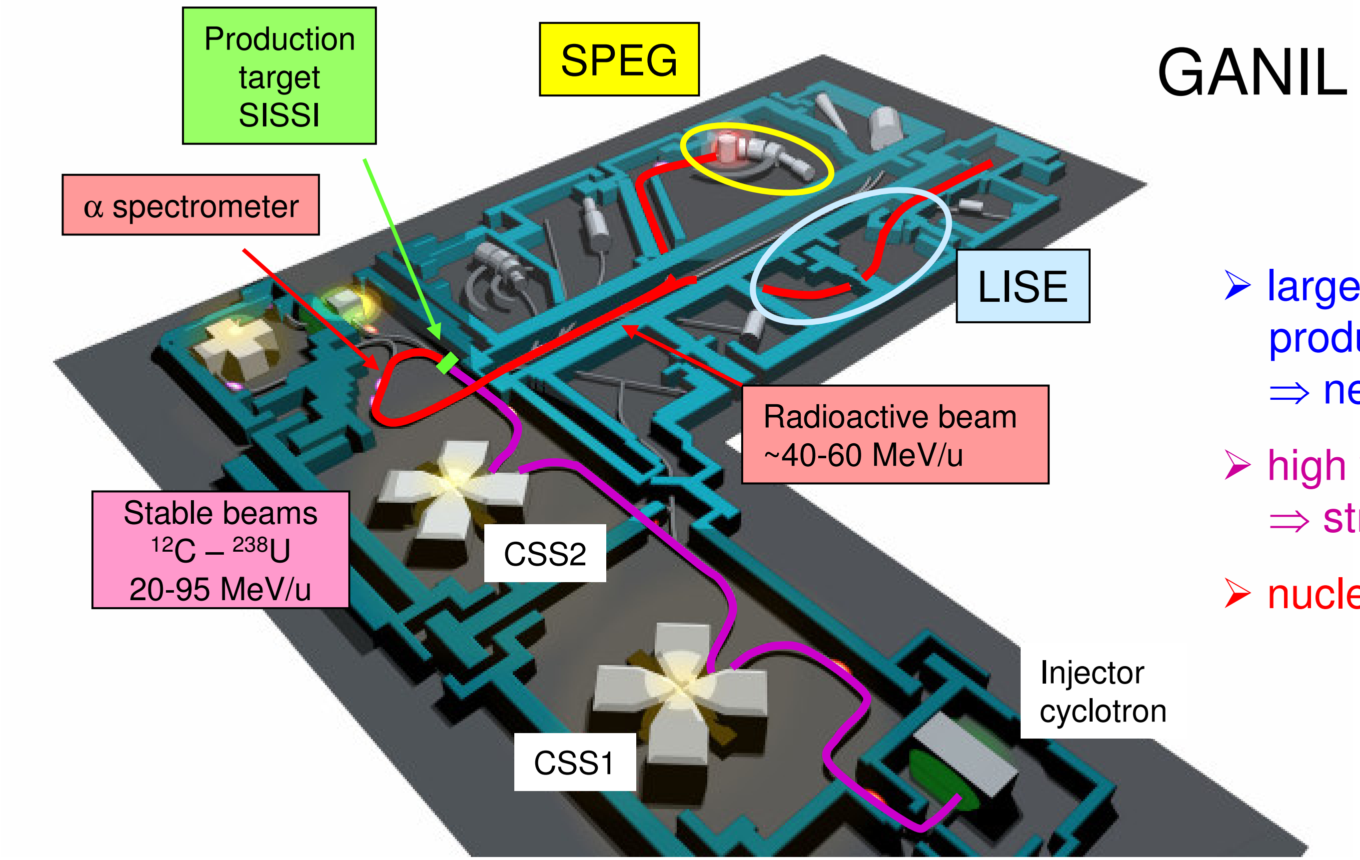

- large number of isotopes produced
  $\Rightarrow$ need for identification
- high velocities
  $\Rightarrow$ strong Doppler effects
- nuclei far from stability

Fragmentation

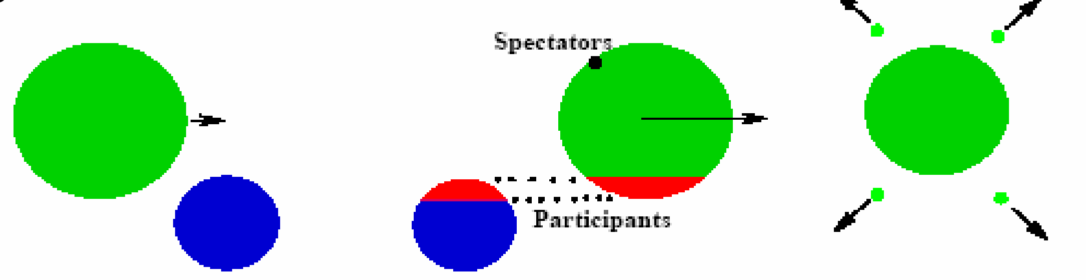

Fast fragmentation beams: separation

Example: LISE

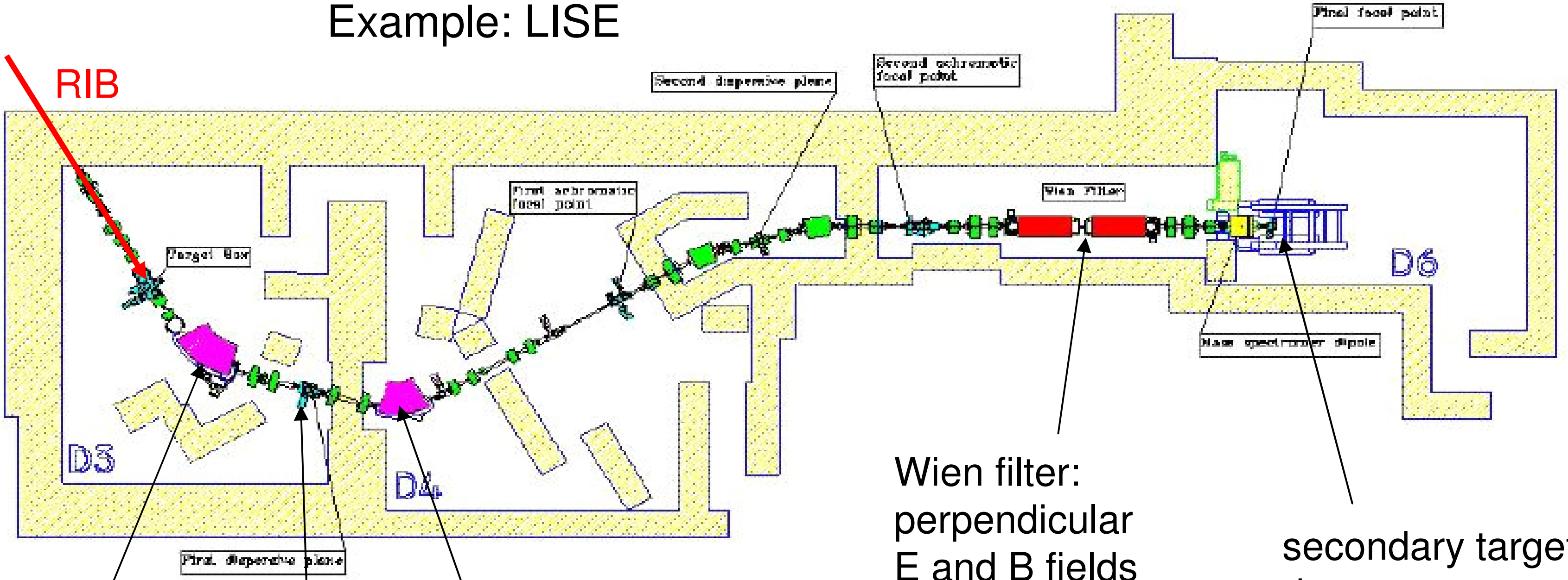

1. Dipole magnet

$$B\rho_1 = \frac{mv}{q}$$

2. Dipole magnet

$$B\rho_2 = \frac{mv}{q}$$

Wien filter:
perpendicular
E and B fields

$$qE = qvB$$

secondary target
detectors

Degrader wedge
different energy loss
for different nuclei

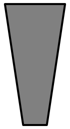

Isomer spectroscopy of ^{72}Kr at LISE

^{78}Kr
70 MeV/u
~10^{12} pps

^{9}Be target

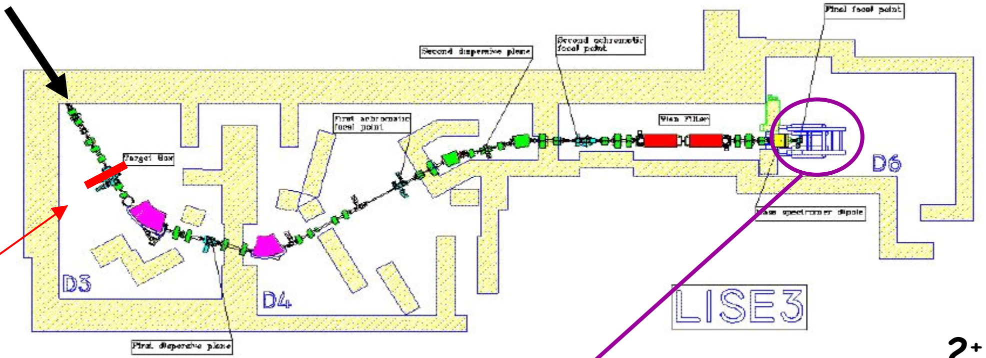

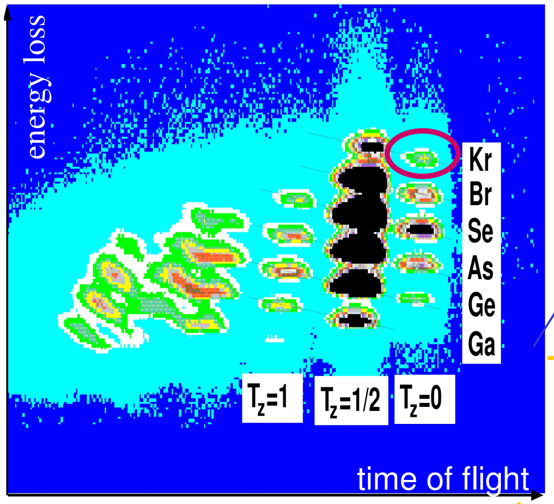

^{72}Kr : ~2 ions/sec

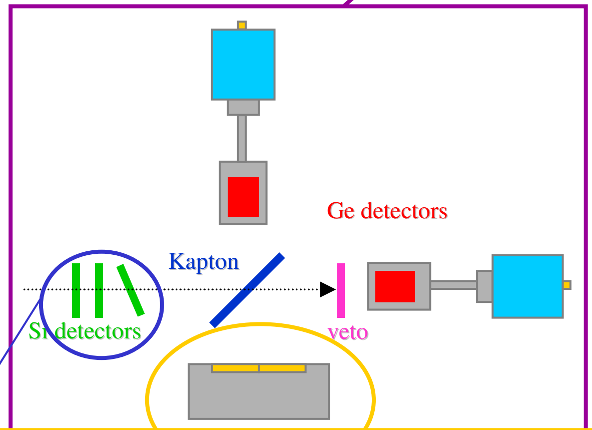

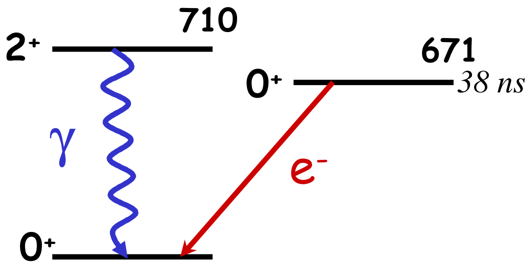

new shape isomer in ^{72}Kr

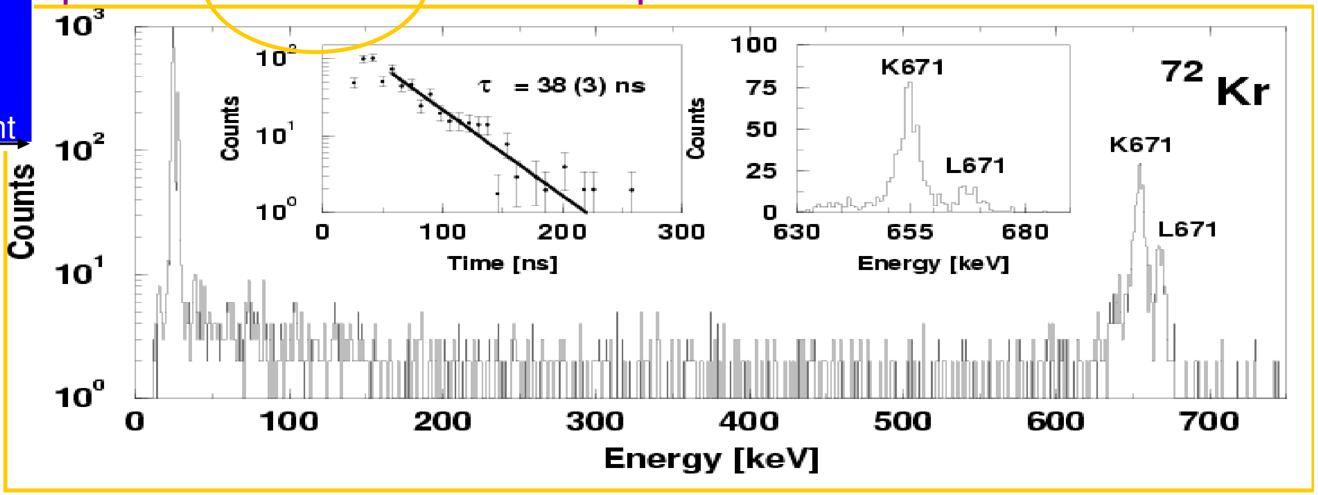

E. Bouchez et al.,
PRL 90, 082502 (2003)

E0 transitions

- electric monopole transitions can occur between states of the same spin and parity in particular $0^+ \rightarrow 0^+$

- E0 transitions are non-radiative:
  only internal conversion or internal pair creation (E >1.022 MeV) possible

- E0 transitions related to changes in the rms radius of the charge distribution (breathing mode)

- monopole matrix element $$\rho = \left\langle 0_f^+ \left| \sum_p \frac{r_p^2}{R^2} \right| 0_i^+ \right\rangle$$

r_p radius vector of the protons
$R = 1.25\ A^{1/3}$ nuclear radius

- example: two 0^+ states of different shapes with mixing

$$|0_i^+\rangle = a|\mathrm{sph}\rangle + b|\mathrm{def}\rangle$$
$$|0_f^+\rangle = -b|\mathrm{sph}\rangle + a|\mathrm{def}\rangle$$

E0 transition strength $\rho^2 \propto a^2 b^2 \beta^4 = a^2(1-a^2)\beta^4$

E0 transitions proceed only in the presence of a sizeable deformation and mixing of components with different $\langle r^2 \rangle$

Systematics of the light krypton isotopes

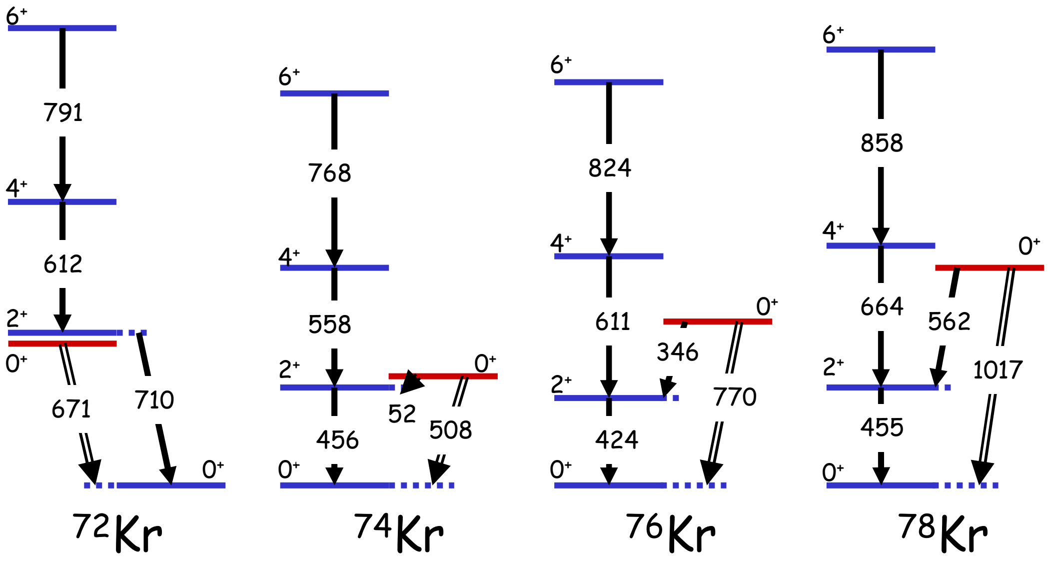

- low-lying 0^+ states
- decay via E0 transitions
- different shapes involved ?

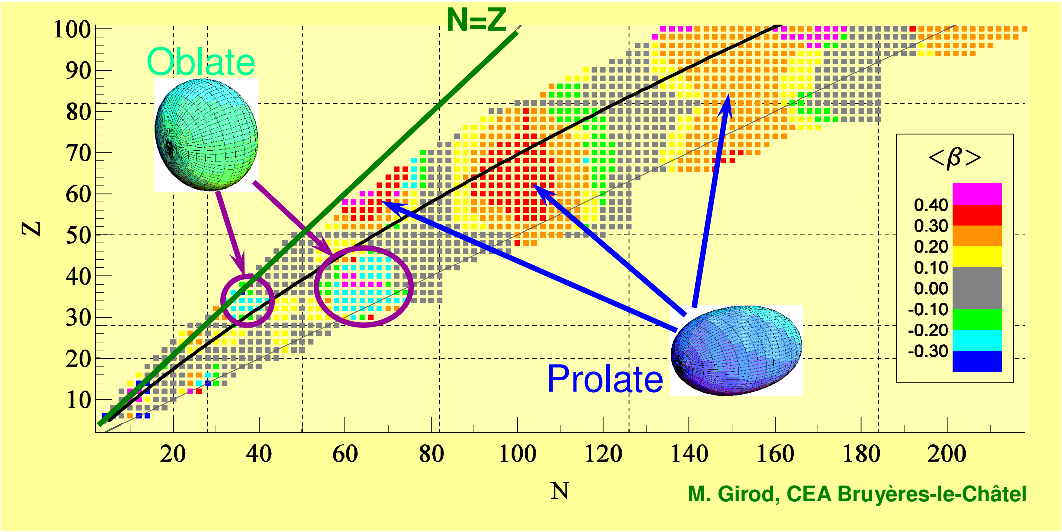

- rotational bands at high spin known to be prolate
- oblate states predicted at low spin

- shape coexistence ?
- mixing ?

Hartree-Fock-Bogoliubov calculation of ground-state shapes

Shape coexistence

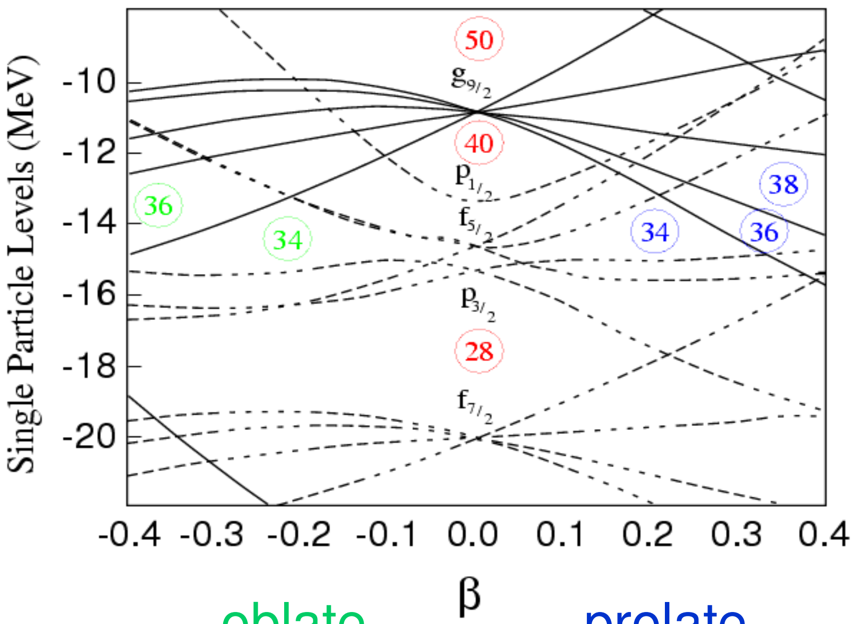

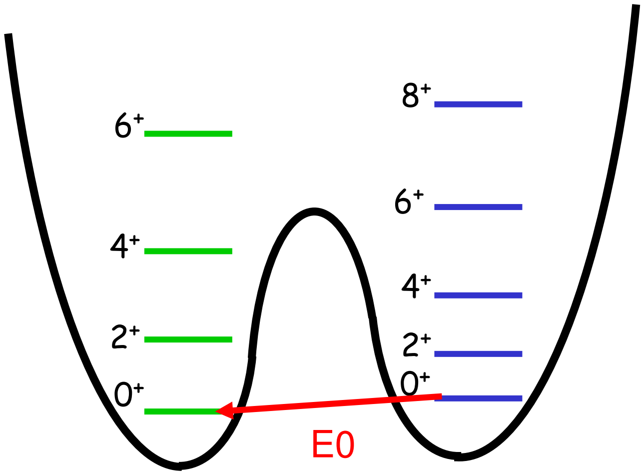

competition of shapes expected in

$^{72}_{36}Kr_{36}$ $^{74}_{36}Kr_{38}$ $^{68}_{34}Se_{34}$ $^{70}_{34}Se_{36}$

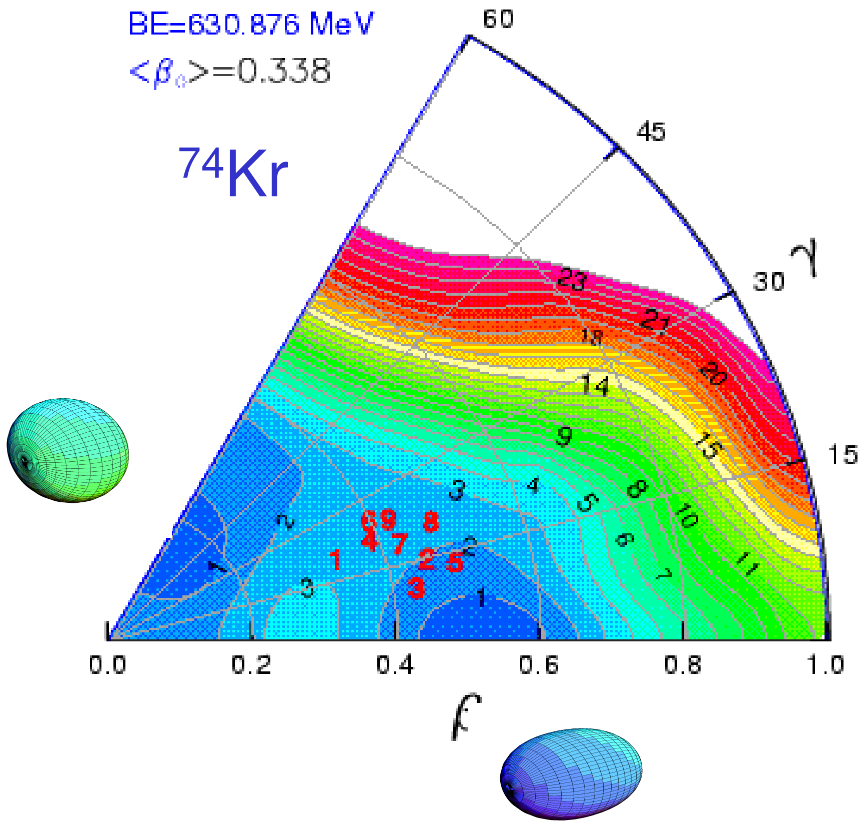

Two-level mixing calculation

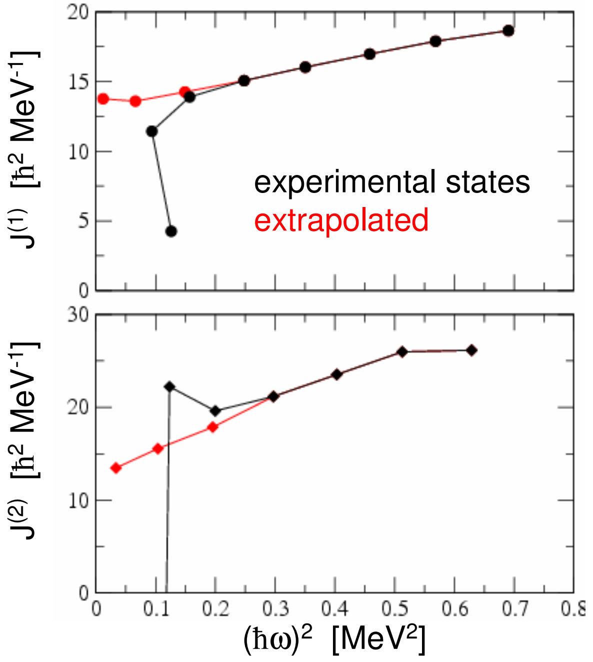

Regular rotational cascade at high spin:

$$E(I) = \frac{\hbar^2}{2\mathcal{J}} I(I+1)$$

Rotational band is distorted at low spin.
⇒ influence of mixing

- ➤Interaction V
- ➤mixing amplitudes α, β

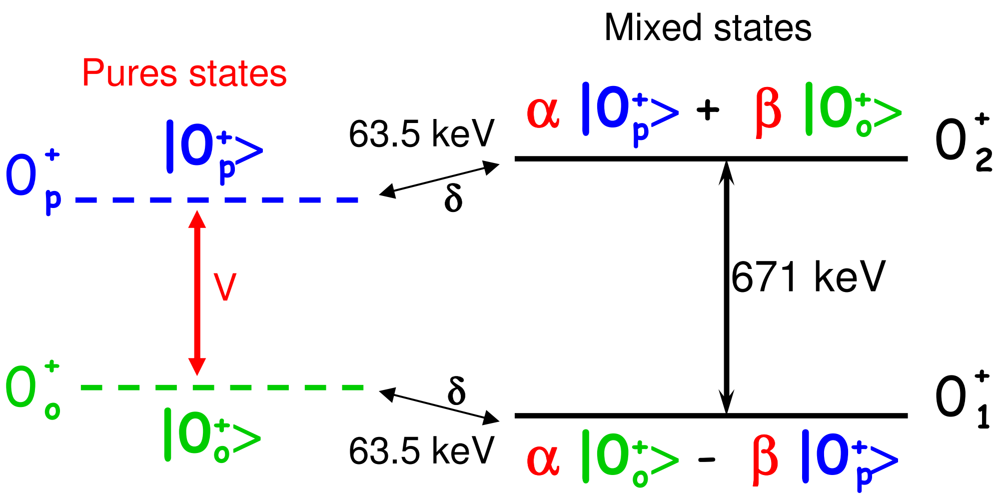

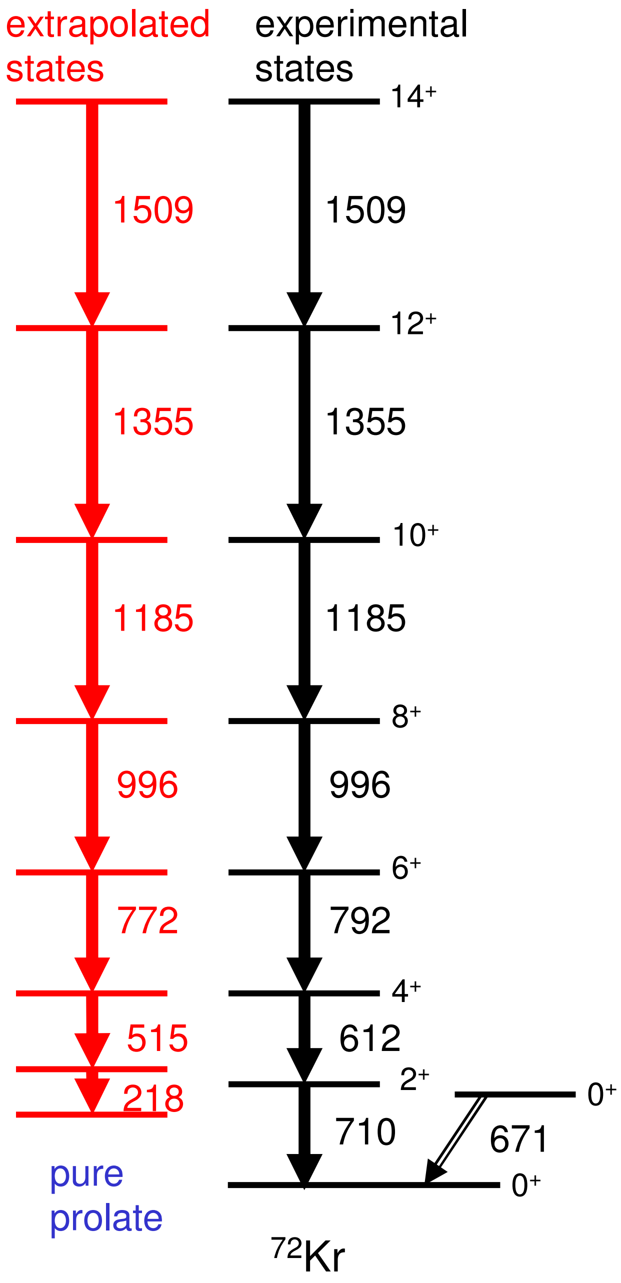

Systematics of the light krypton isotopes

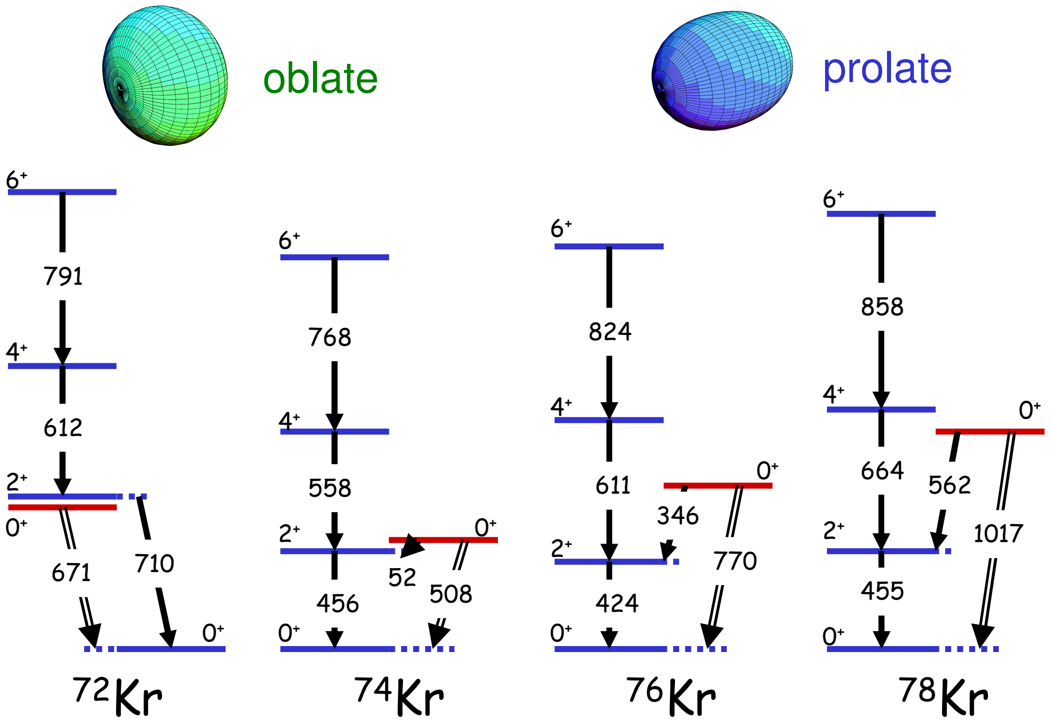

- energy of excited 0^+ states
- E0 transitions strengths
- mixing amplitudes

Inversion of the ground-state shape for ^{72}Kr

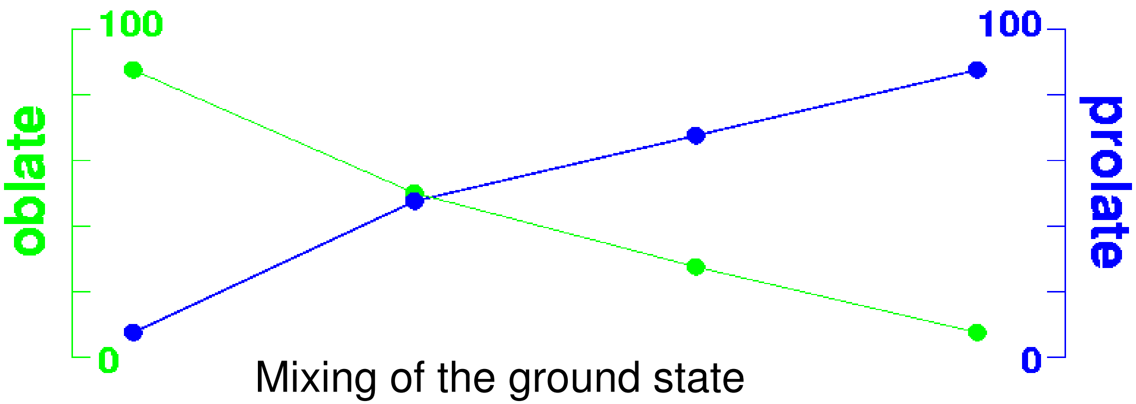

can we prove this scenario directly ?
⇒ Coulomb excitation

E. Bouchez et al., PRL 90, 082502 (2003)

Coulomb excitation

Nuclear excitation by electromagnetic field acting between nuclei.

Trajectories are hyperbolas $\frac{x^2}{a^2} - \frac{y^2}{b^2} = 1$

(Rutherford scattering)

a $\propto$ beam energy
b = impact parameter

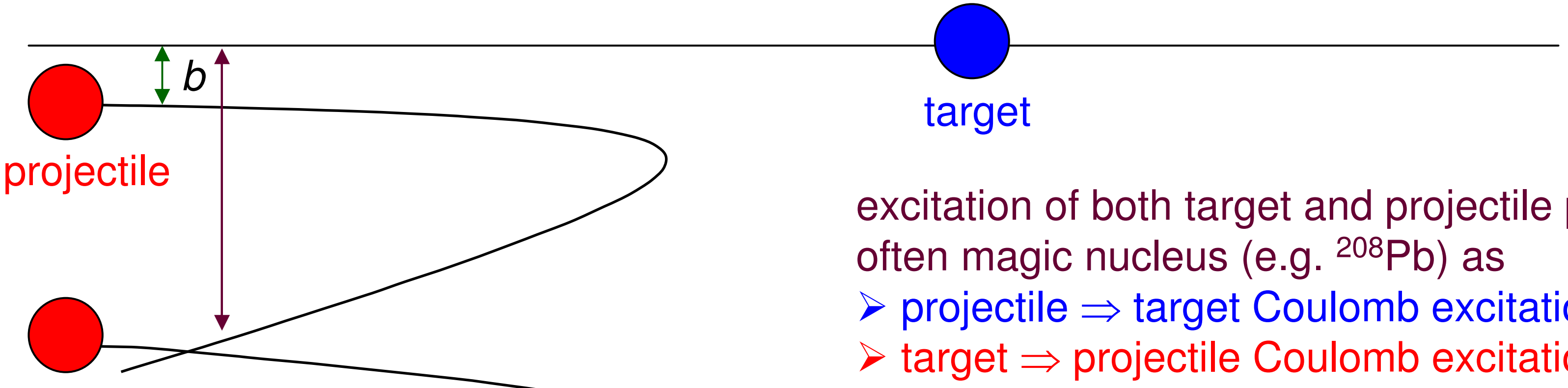

excitation of both target and projectile possible
often magic nucleus (e.g. ^{208}Pb) as
- projectile $\Rightarrow$ target Coulomb excitation
- target $\Rightarrow$ projectile Coulomb excitation
  important technique for radioactive beams

small impact parameter
- back scattering
- close approach
- strong EM field

large impact parameter
- forward scattering
- large distance
- weak EM field

“safe” Coulomb excitation at low energy = purely electromagnetic process
safe condition: distance of closest approach $d > 1.25\left(A_P^{1/3} + A_T^{1/3}\right) + 5 \text{ fm}$
$\Rightarrow$ choose beam energy and scattering angle (i.e. impact parameter) accordingly

Reorientation effect

1st order:

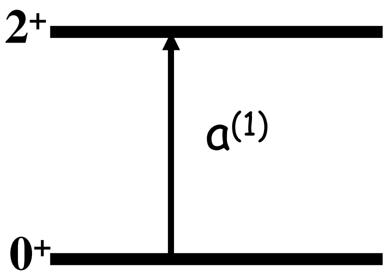

$P_{i\to f} = P^{(1)} \propto B(E2)\, Z_{target} \propto \beta^2$

2nd order:

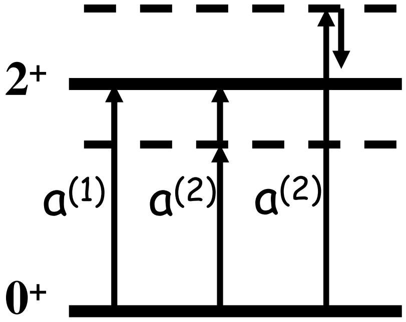

$P_{i\to f} = P^{(1)} + P^{(2)} + P^{(1,2)}$

reorientation effect

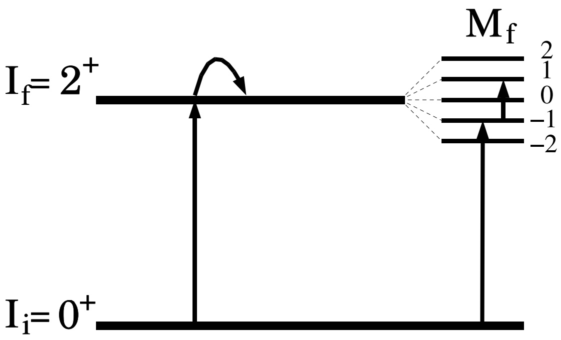

$P_{i\to f} = P^{(1)} + P^{(2)} + P^{(1,2)} = f(Q_0)$

Cross section

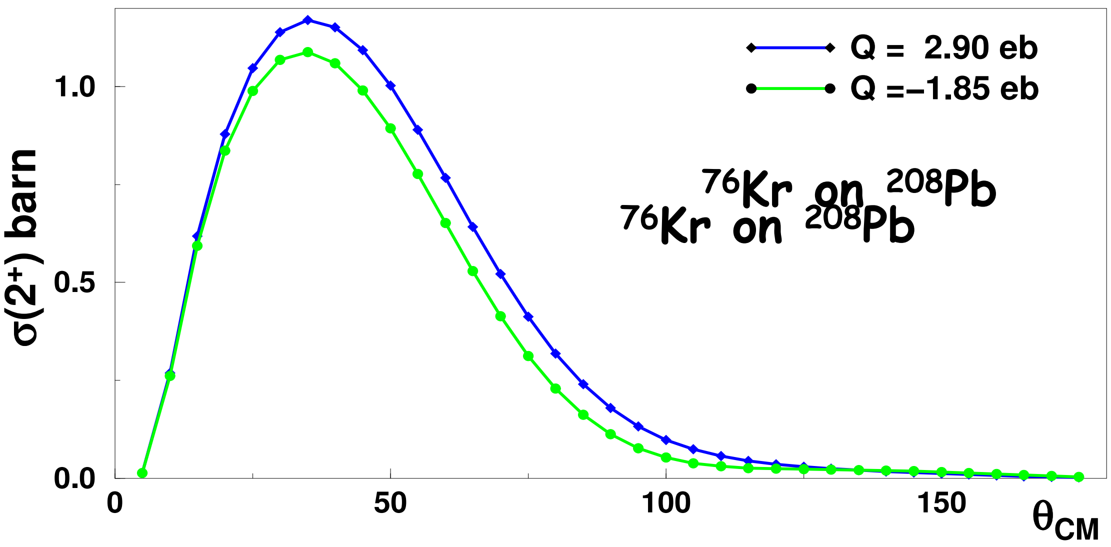

Radioactive ion beams: Isotope separation on-line (ISOL)

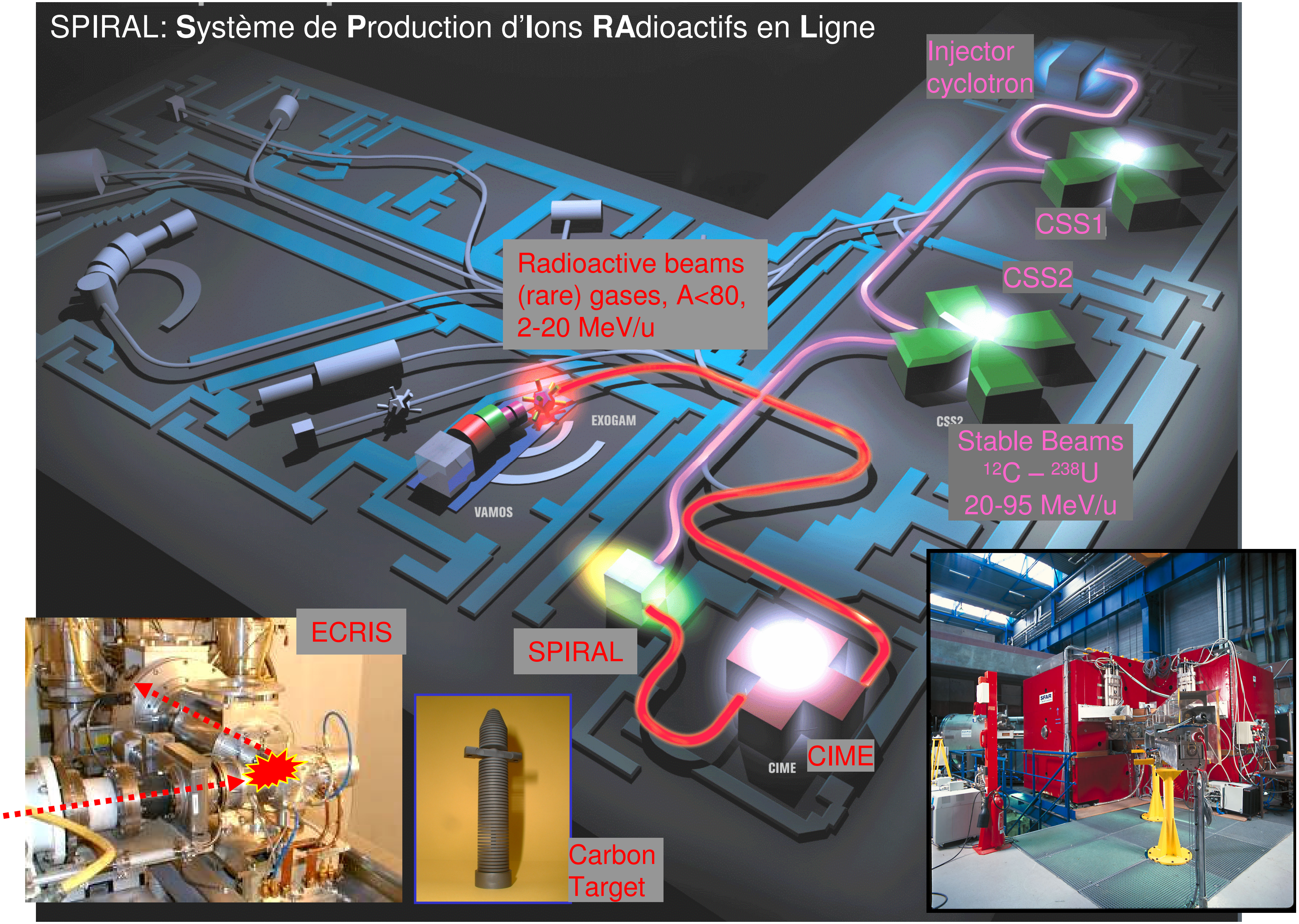

Coulomb excitation of $^{74,76}Kr$

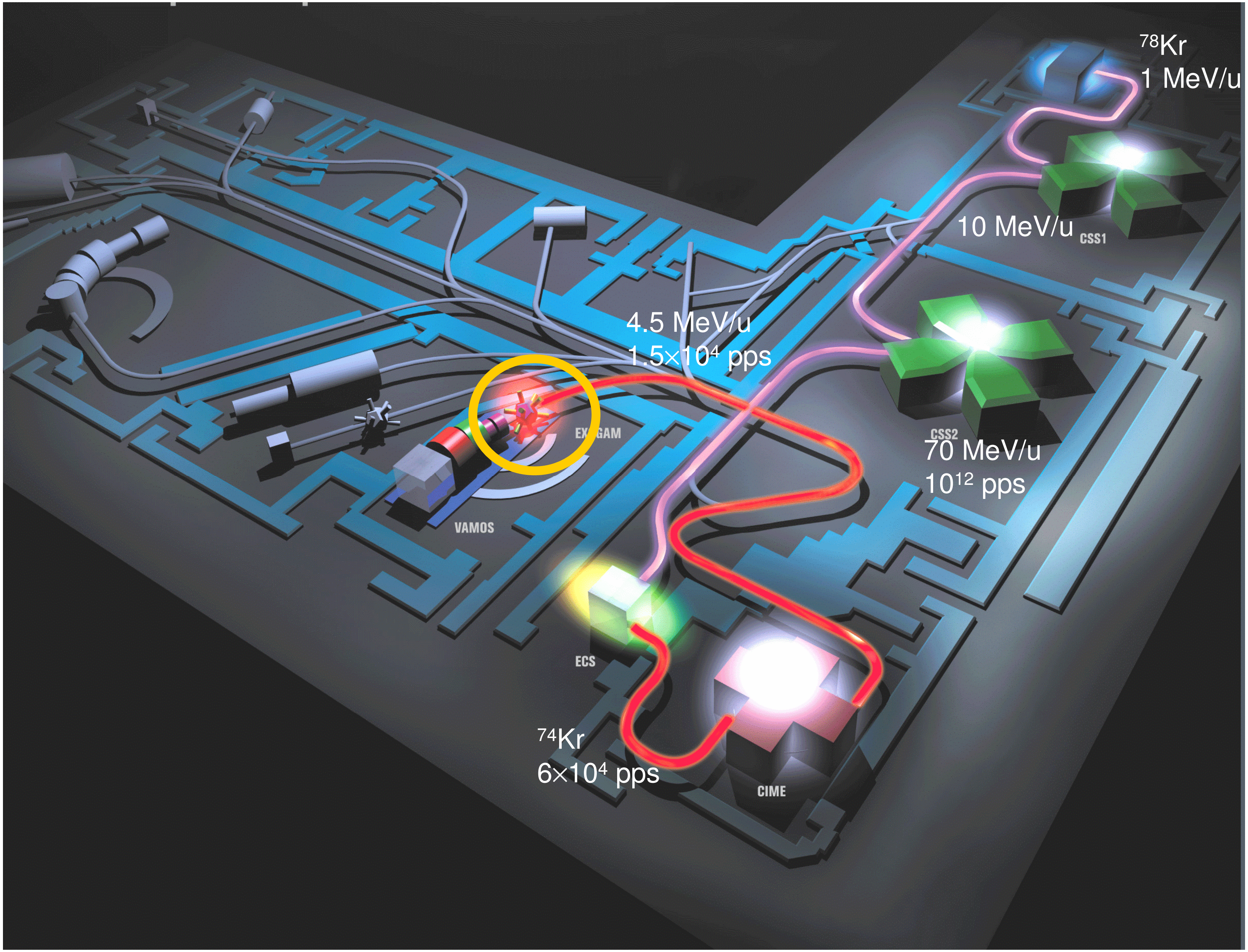

EXOGAM

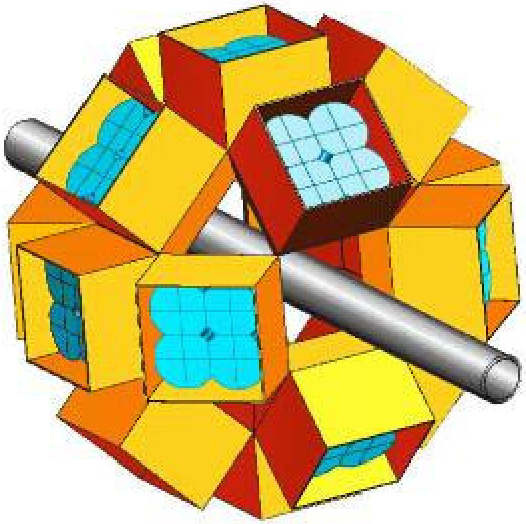

16 large Ge Clover detectors
4×4 segmented
photopeak efficiency $\varepsilon = 20\%$

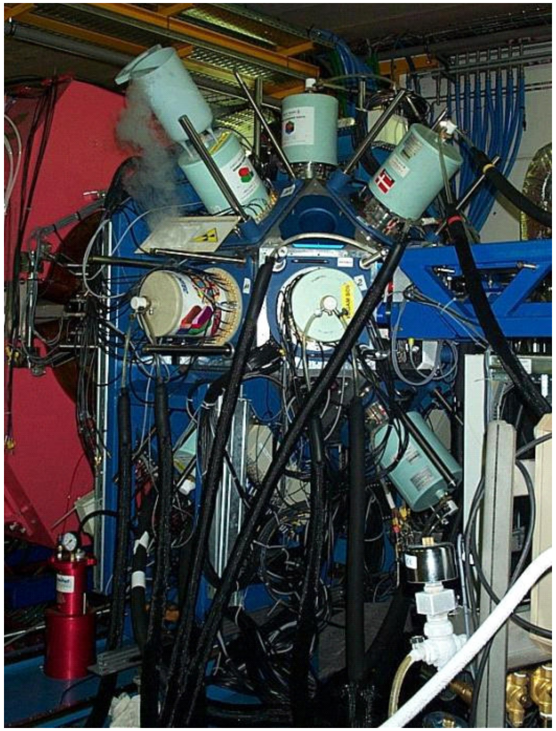

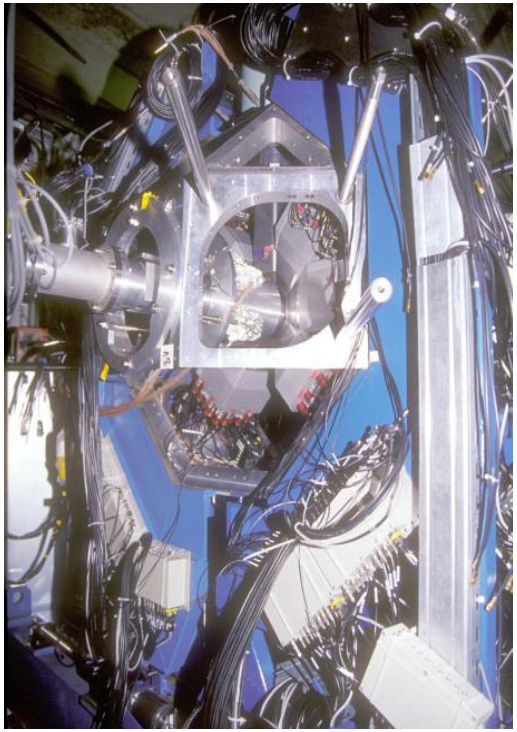

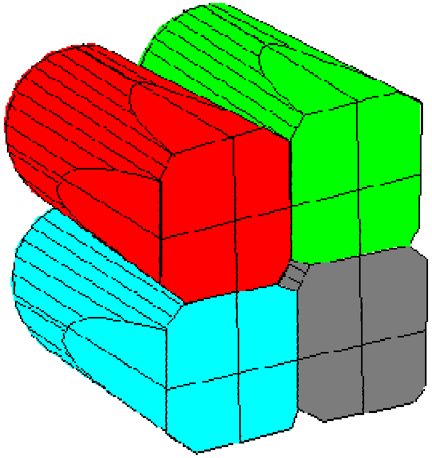

Double-sided Si detector
48 rings $\times$ 16 sectors

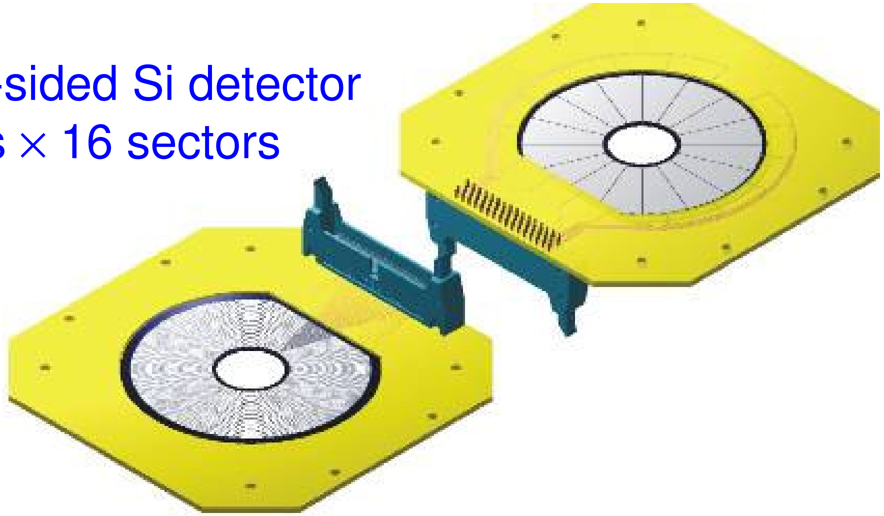

Coulomb excitation of ^{74}Kr and ^{76}Kr

SPIRAL beams
^{76}Kr 5×10^5 pps
^{74}Kr 10^4 pps

4.5 A MeV

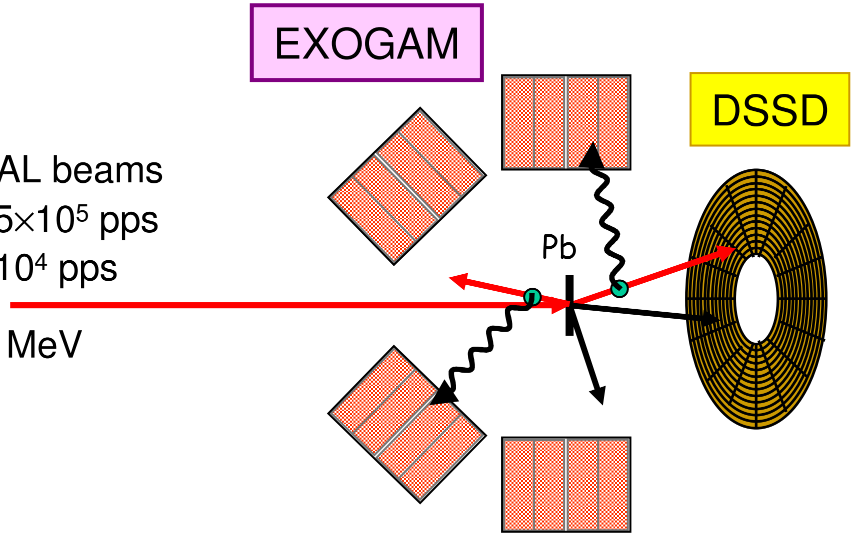

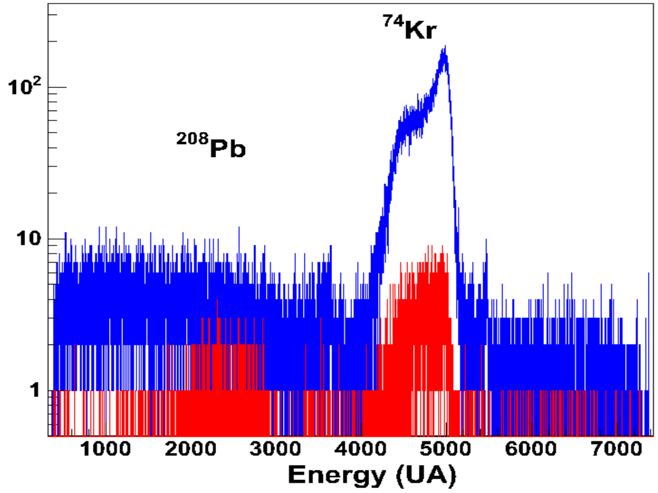

Differential Coulomb excitation cross section for 35° < θ_{cm} < 130°

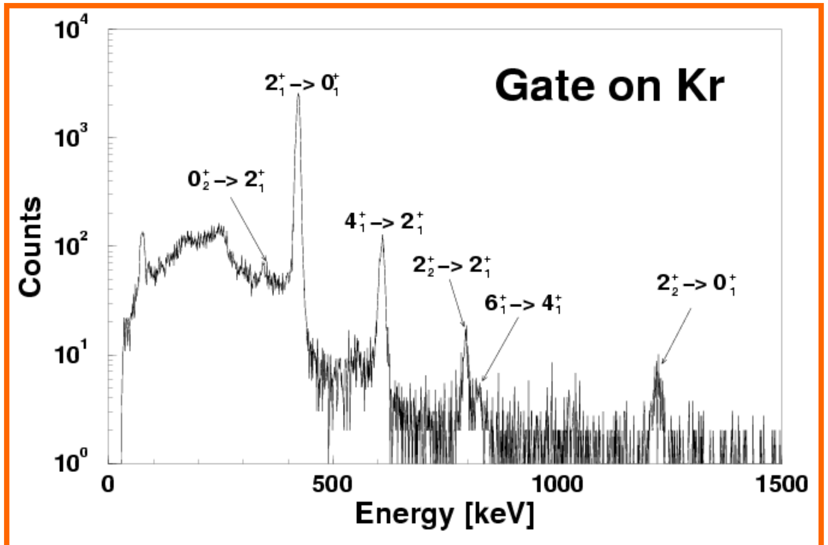

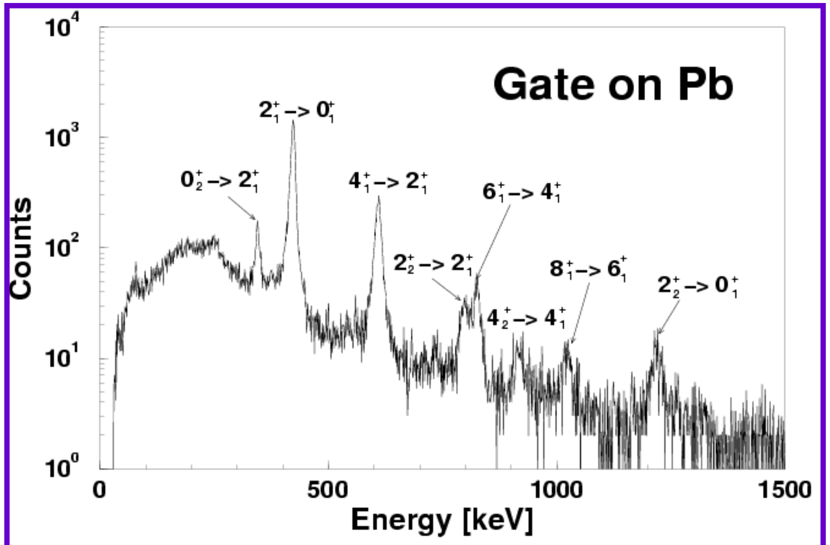

A. Görgen et al., Acta Phys. Pol. B 36, 1281 (2005)

Coulomb excitation analysis : GOSIA*

*D. Cline, C.Y. Wu, T. Czosnyka; Univ. of Rochester

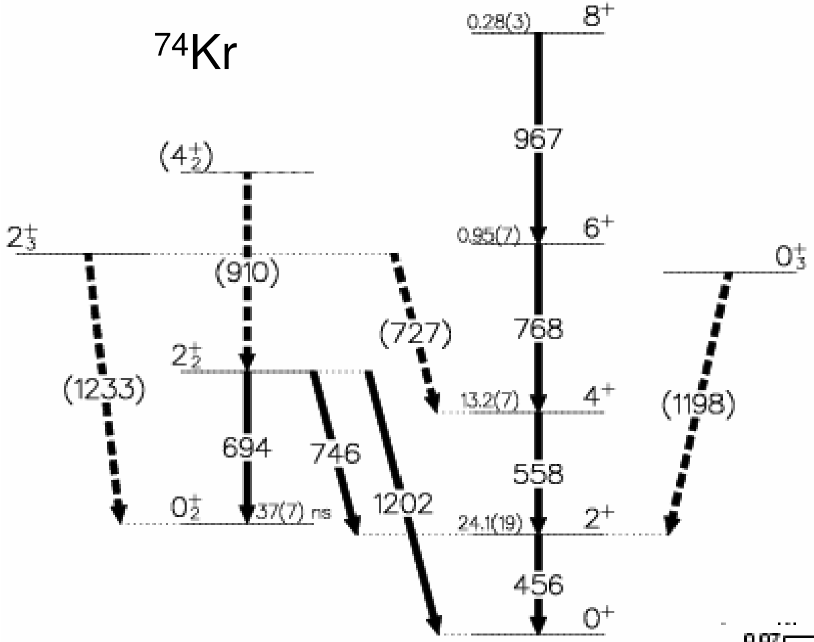

- γ yields as function of scattering angle: differential cross section
- least squares fit of ~ 30 matrix elements (transitional and diagonal)
- experimental spectroscopic data
  - lifetimes
  - branching ratios
  - mixing ratios

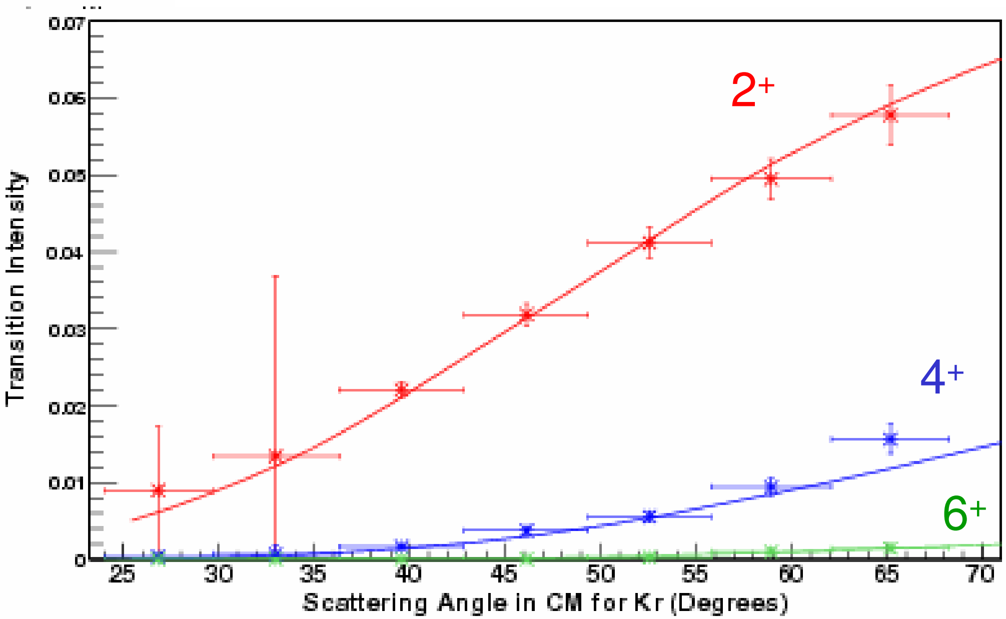

dapnia
cea
saclay

Quadrupole moments in ^{74}Kr and ^{76}Kr

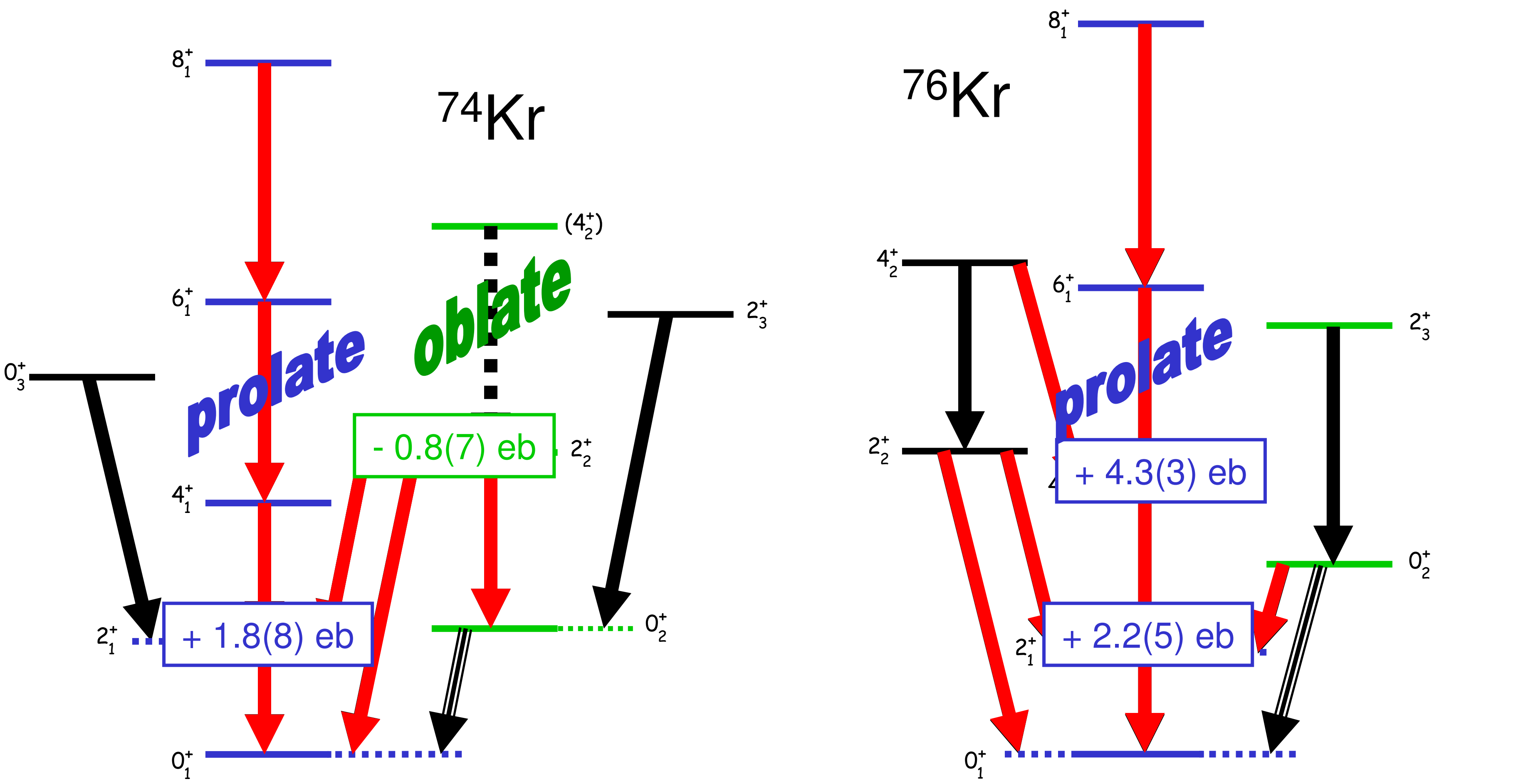

A. Görgen et al.,
Acta Phys. Pol. B 36, 1281 (2005)

- transitional matrix elements $\rightarrow$ B(E2)
- diagonal matrix elements $\rightarrow$ static quadrupole moments

Low-energy vs. relativistic Coulomb excitation

low-energy Coulomb excitation
- energy well below the Coulomb barrier: < 5MeV/u
- purely electromagnetic process
- multiple-step excitation
- can populate high-spin states> up to ~30 ħ in actinides
- sensitive to static quadrupole moments (reorientation effect)
- limited to stable and moderately exotic nuclei

relativistic Coulomb excitation
- energy well above the Coulomb barrier: ~50 - 500 MeV/u
- nuclear contribution
- single-step excitation
- populates 2^+ state only
- sensitive to transitional matrix elements (i.e. B(E2) values)
- tool to study very exotic nuclei

RISING at GSI

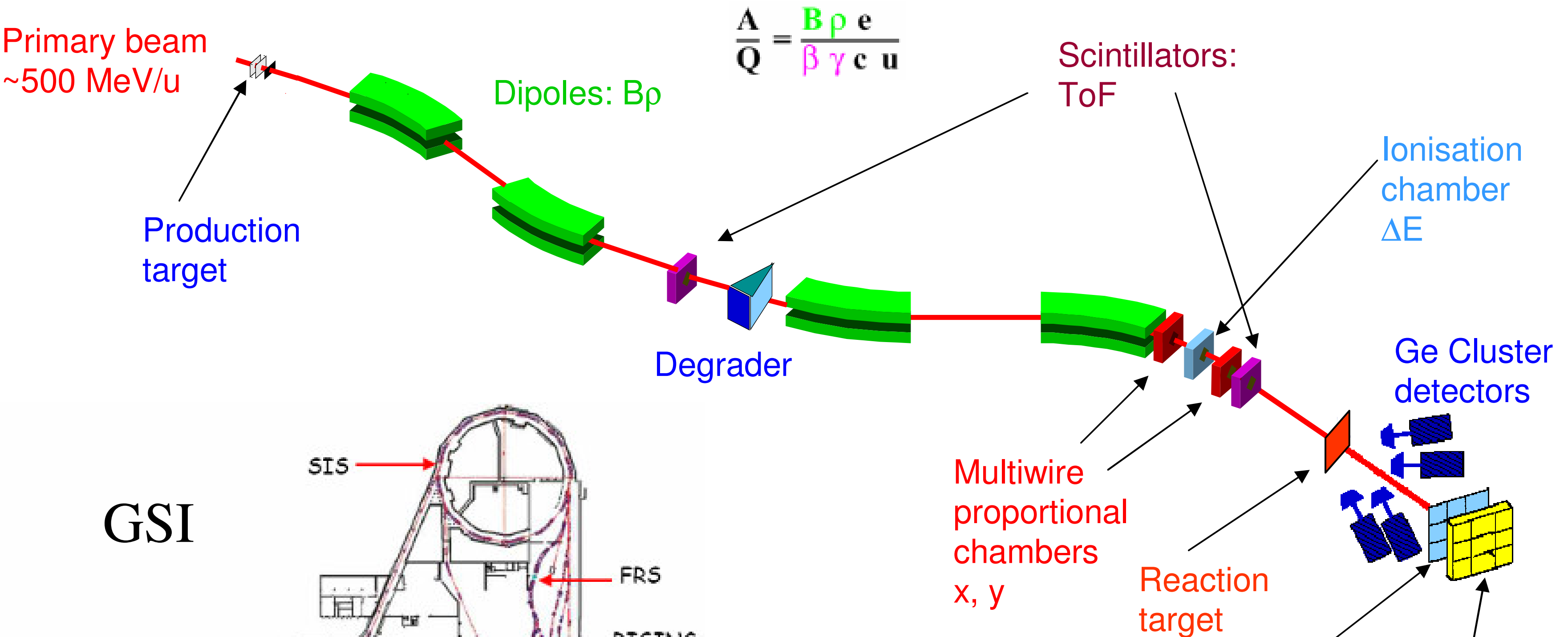

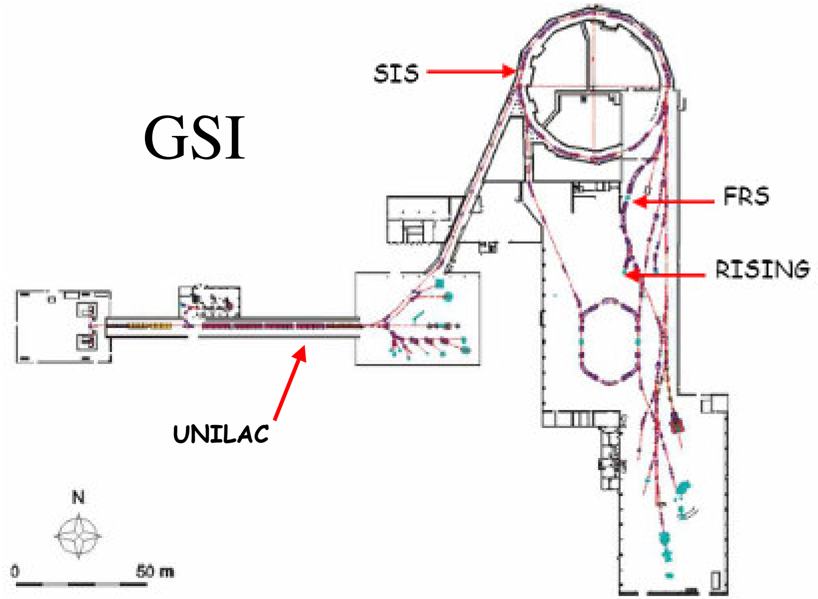

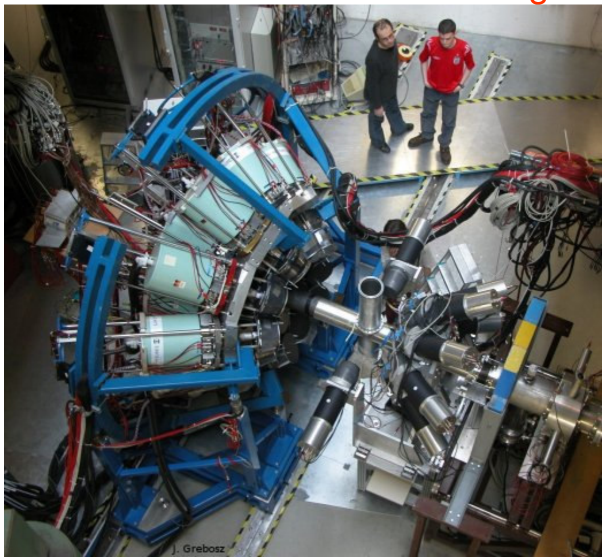

Relativistic Coulomb excitation of $^{54,56,58}Cr$

Identification before the secondary target

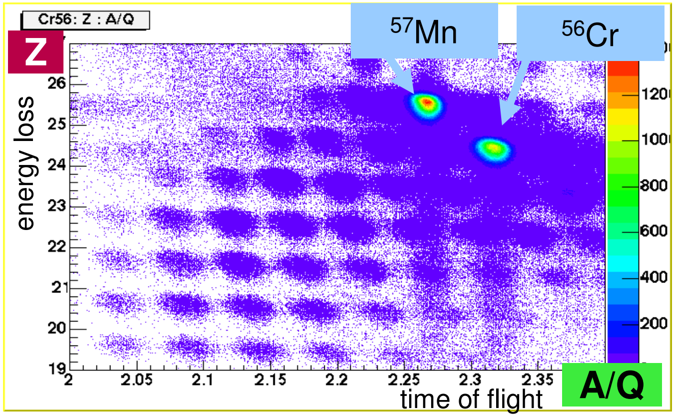

after secondary target

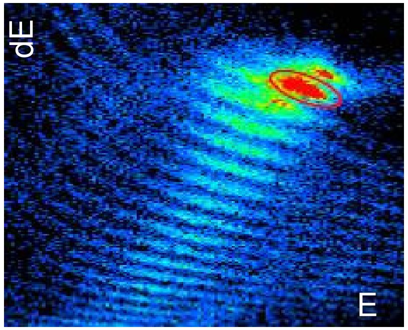

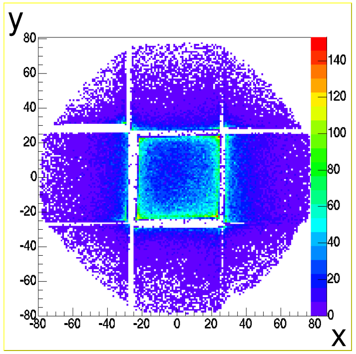

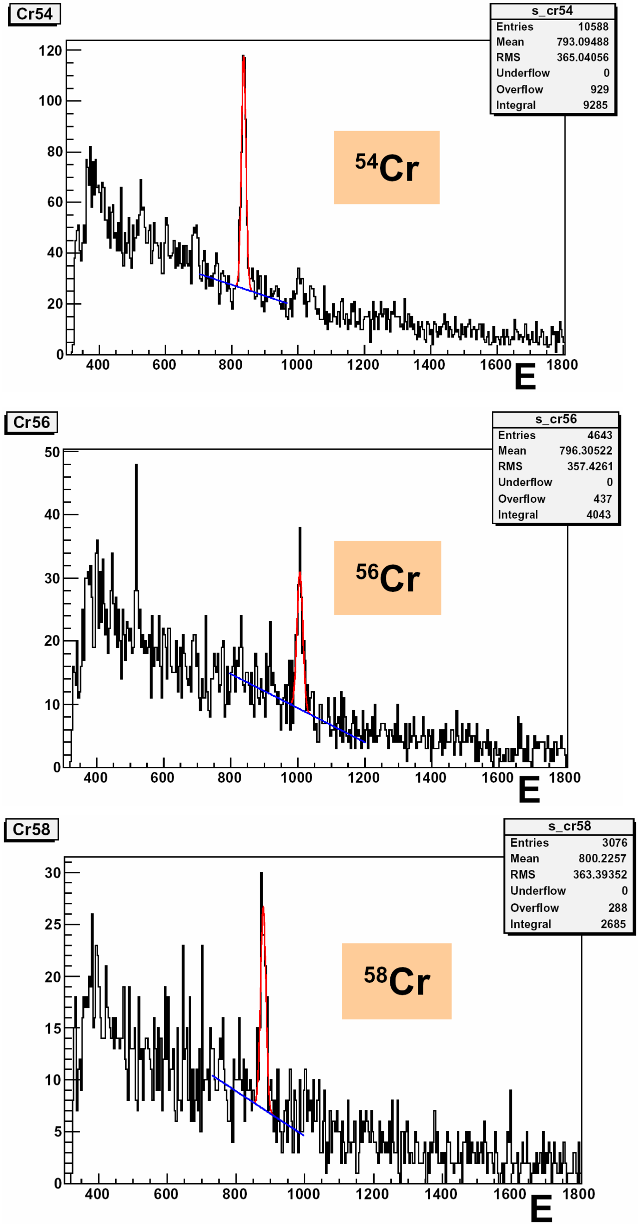

- identification of nuclide before and after the secondary target to select Coulomb excitation events
- tracking of incoming and outgoing particles to determine scattering angle and perform Doppler correction (v/c=0.43)

A. Bürger et al., Phys. Lett B 622, 29 (2005)

dapnia SPhN
cea
saclay

Systematics of the Cr isotopes

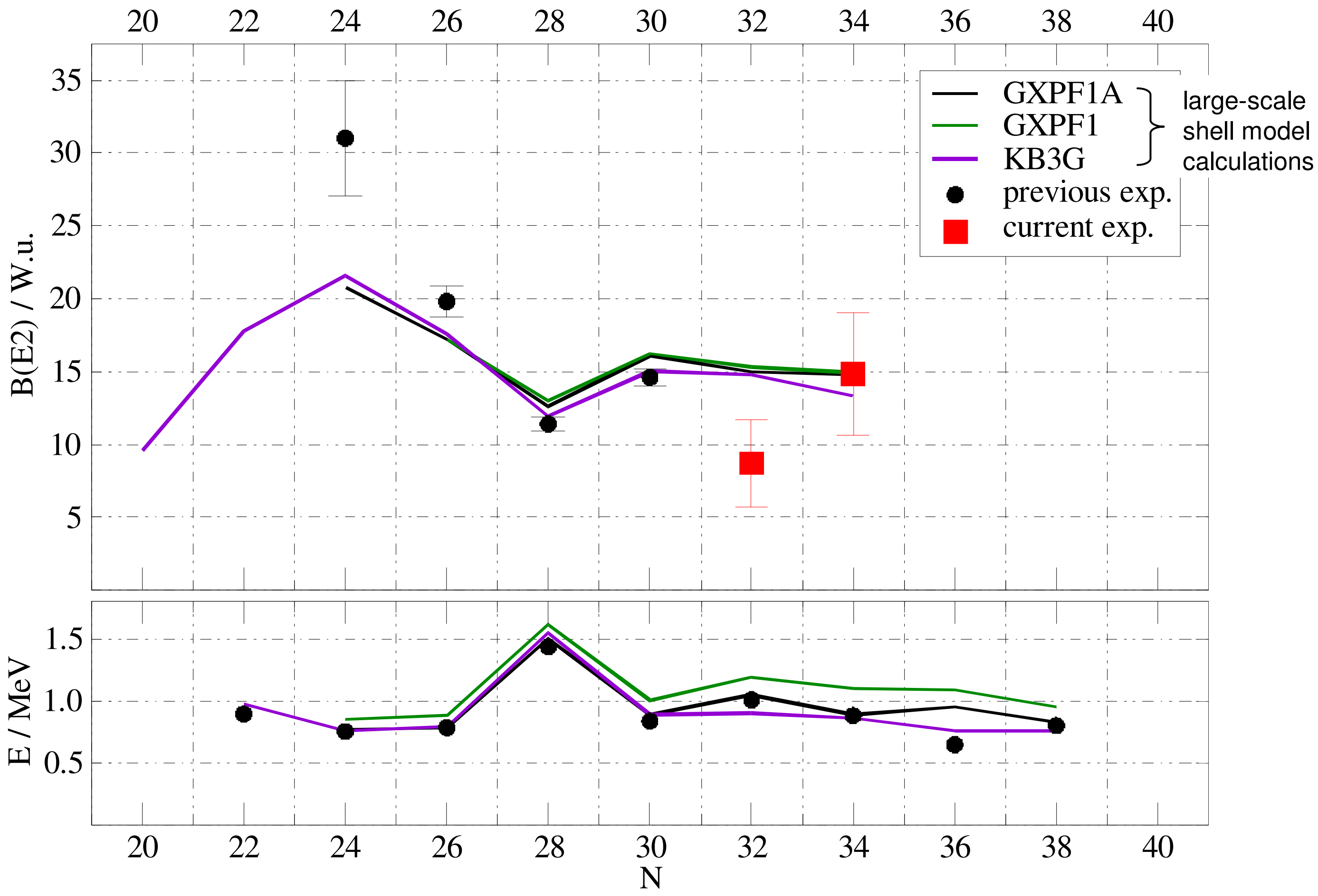

- ➢ significant lower collectivity for ^{56}Cr
- ➢ sub-shell closure at N=32
- ➢ evolution of shell structure for exotic nuclei
- ➢ new magic numbers for neutron-rich nuclei

Gamma-ray tracking

Compton Shielded Ge

ε_{ph}	~ 10%
N_{det}	~ 100

Ω ~40%

large opening angle means poor energy resolution at high recoil velocity

Ge Sphere

ε_{ph}	~ 50%
N_{det}	~ 1000

too many detectors are needed to avoid summing effects

Ge Tracking Array

ε_{ph}	~ 50%
N_{det}	~ 100

Ω ~80%

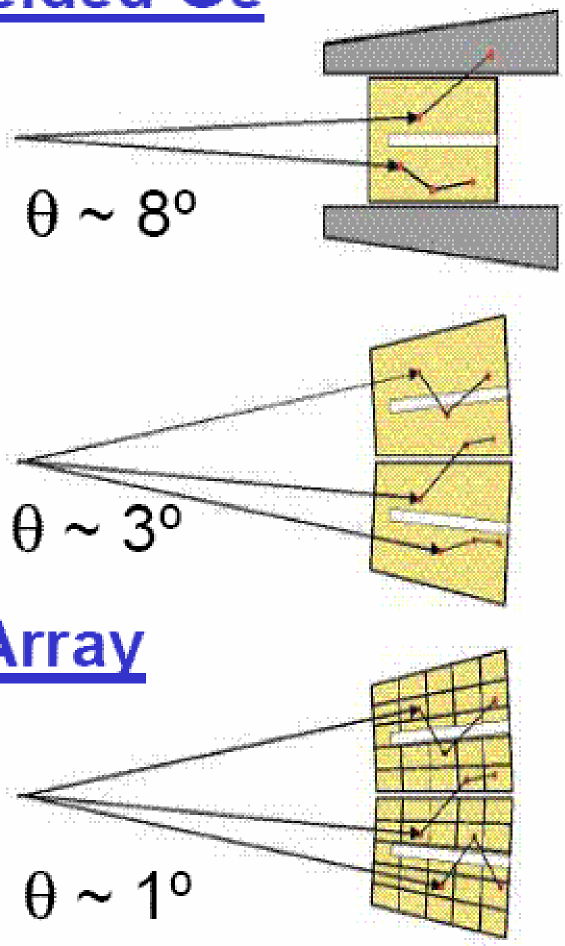

Combination of:

- segmented detectors
- digital electronics
- pulse processing
- tracking the γ-rays

Position-sensitive segmented Ge detector

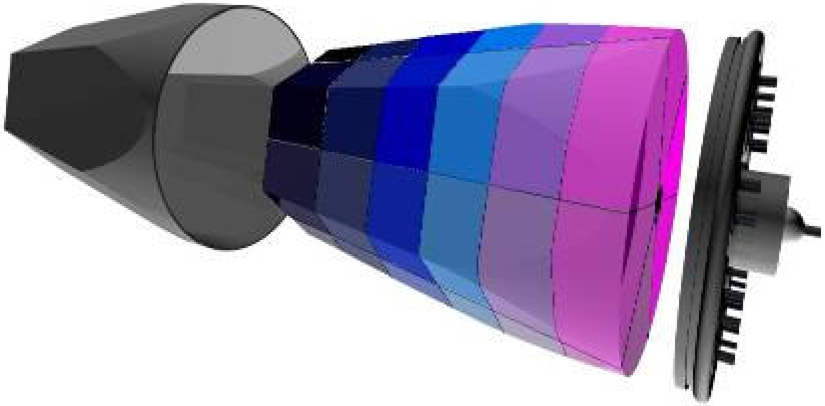

- encapsulated, coaxial Ge monocrystal
- 6 x 6 fold “electrical” segmentation
- “hexaconical” tapered shape

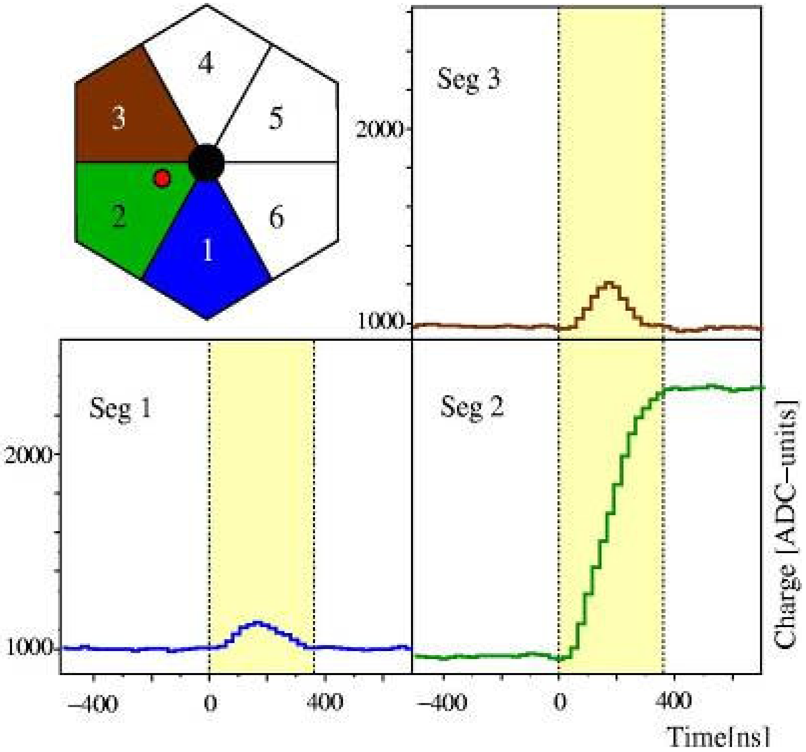

Position information from pulse-shapes :

- signal rise time ➔ radius
- “image charges” ➔ azimuth & depth

⇒ position determination in 3 dimensions
($\Delta x = \Delta y = \Delta z$ ~ 2-3 mm)

Gamma-ray tracking

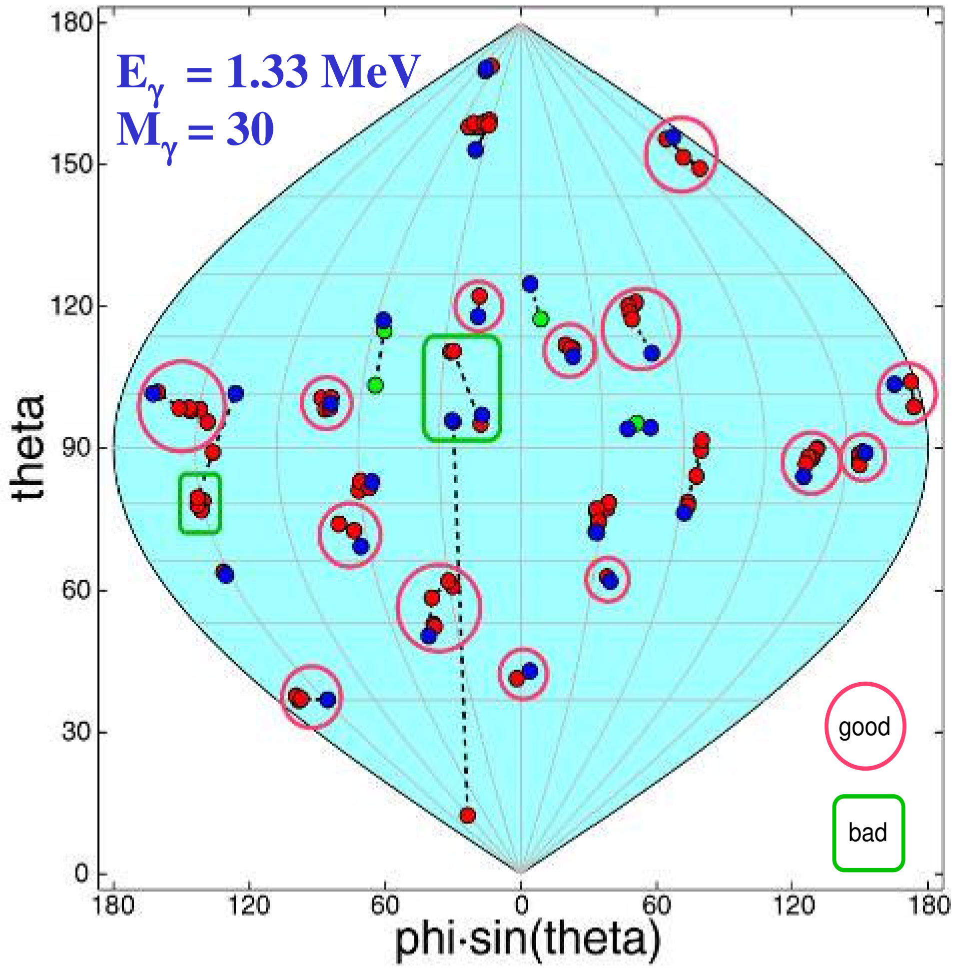

$$E_{\gamma'} = \frac{E_\gamma}{1 + \frac{E_\gamma}{m_0 c^2}(1 - \cos\vartheta)}$$

"Clusterisation" algorithm :

- Identify interaction point clusters
- Validate Clusters using the energy-angle relationship for Compton scattering
- check complete reconstruction

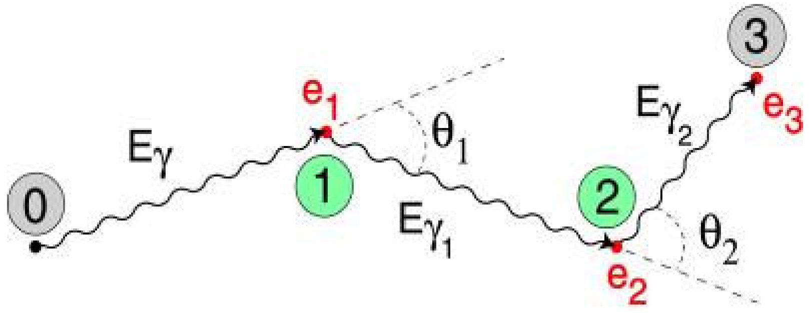

Look for a χ^2 minimum in the N! permutations of the interaction points

0123	0132
0231	0213
0312	0321

AGATA

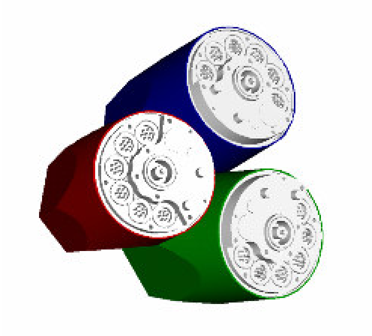

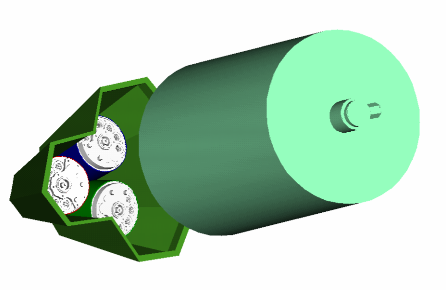

triple-cluster module:
3 slightly different
asymmetric crystals,
36-fold segmented,
in a common cryostat
(tests Aug./Sept. 2005)

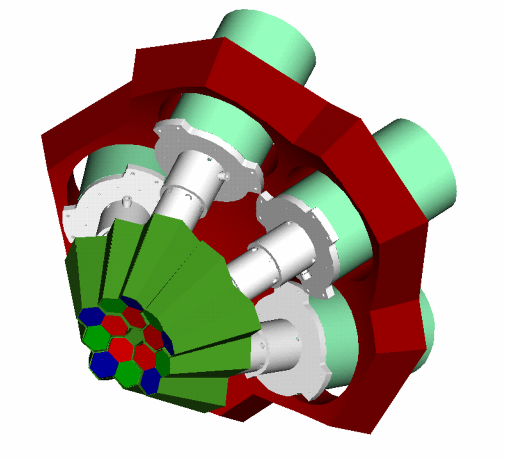

AGATA demonstrator
result of R&D 2003-2008

5 triple-cluster modules
- 36-fold segmented crystals
- 540 segments
- 555 digital-channels
- Eff. 3 – 8 % @ $M_g = 1$
- Eff. 2 – 4 % @ $M_g = 30$

Full ACQ
with on line PSA and γ-ray tracking

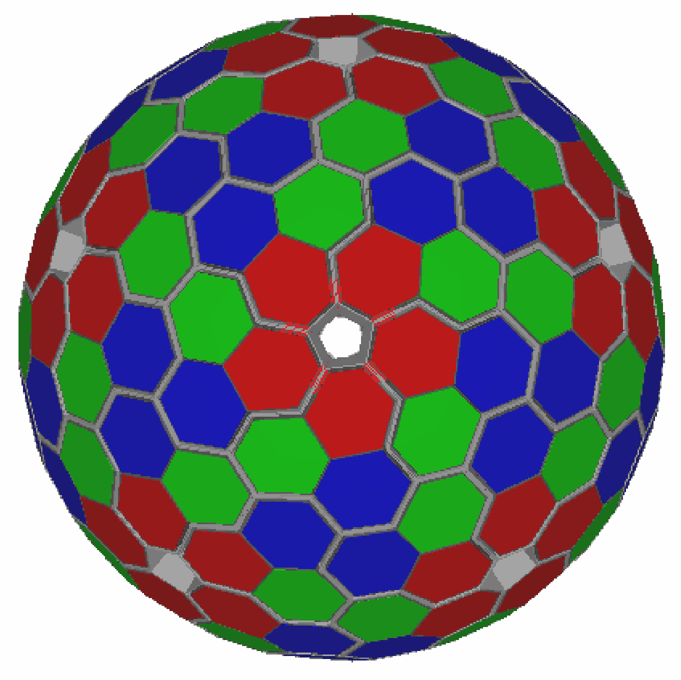

Full AGATA (~2015)
180 Ge crystals
82% solid angle coverage
6480 segments
362 kg germanium
inner radius: 23 cm
singles rate ~50 kHz
6660 digital electronics channels
on-line PSA and tracking
efficiency: 43% (M_γ=1), 28% (M_γ=30)
peak/total: 58% (M_γ=1), 49% (M_γ=30)

Performance of γ-ray tracking

experimental conditions

- low intensity beam
- high background
- large Doppler broadening
- high counting rates
- high γ-ray multiplicity

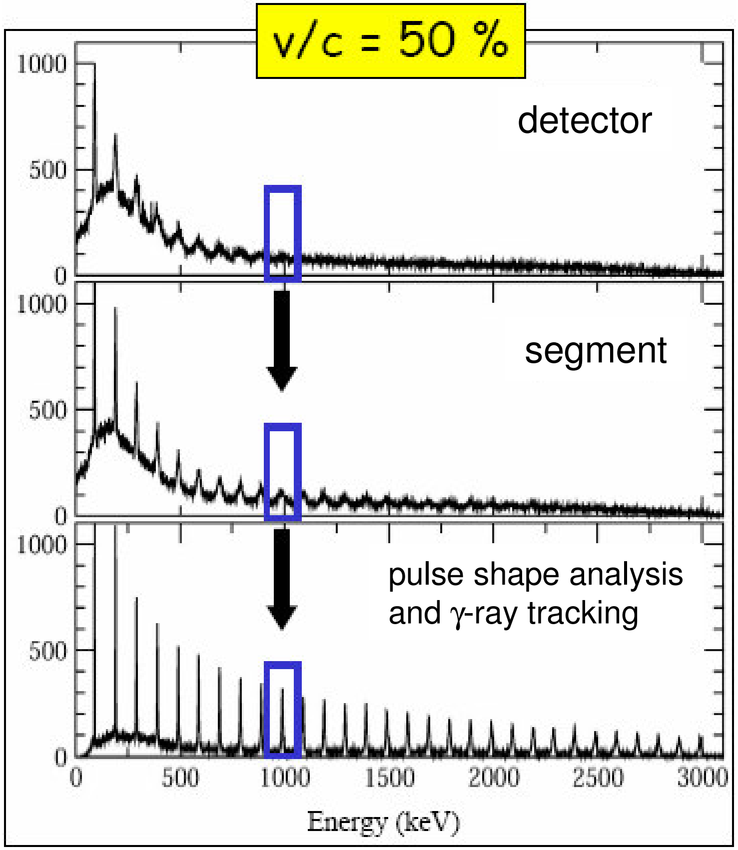

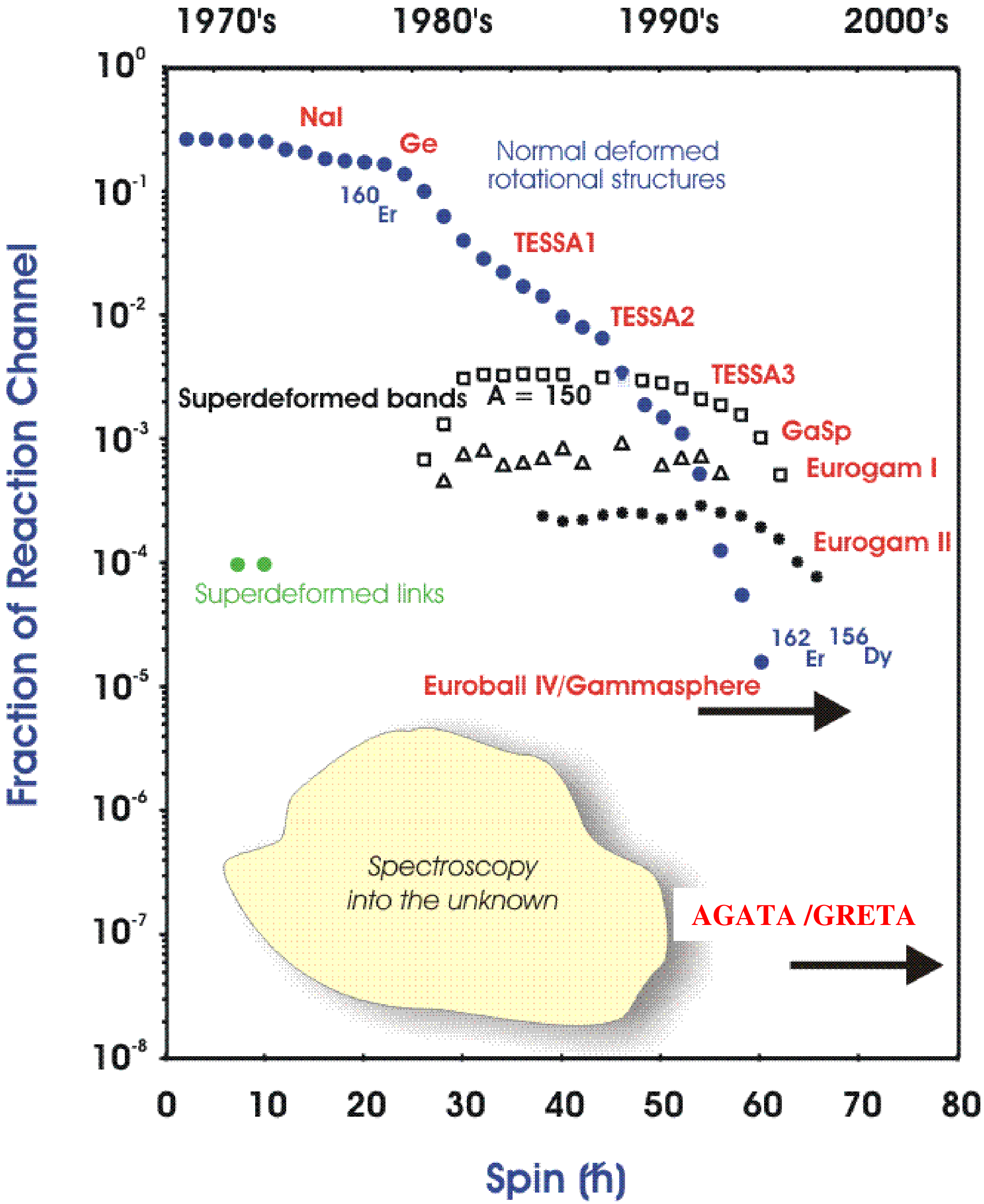

The nucleus is always full of surprises

Instrumentation advances ⇔ New Science

fin